Mathematical Statistician and Engineering Applications
ISSN: 2094-0343
2326-9865

A Review on Glass Failuer Analysis under Loading Condition

Akshay Sirsath
Department of Mechanical Engineering, MIT School of Engineering, MIT-ADT University, Pune, India
akshaysirsath30@gmail.com

Prof. Dr. Anurag Nema
Department of Mechanical Engineering, MIT School of Engineering, MIT-ADT University, Pune, India
anurag.nema@mituniversity.edu.in

Dhiraj Gotekar
People Leader, Whirlpool Corporation, Pune, India

Satadru Bera
Senior CAE Specialist, Whirlpool Corporation, Pune, India

Article Info
Page Number: 9340 - 9355
Publication Issue:
Vol 71 No. 4 (2022)

Article History
Article Received: *15 September 2022*
Revised: *25 October 2022*
Accepted: *14 November 2022*
Publication: *21 December 2022*

Abstract
Glass is used in many kitchen appliances, including doors, HMI consoles, and other components. While being transported and handled from the warehouse to the homes of customers, glass has a possibility to break. Predicting glass failure during the virtual validation phase of product development is difficult. This study offers a review on the glass failure analysis and also predict' s glass failure under the Three Point Bend Test during transit and handling. For this it is essential to study glass behaviors. To increase model quality and failure predictability.

Keywords— Break, Glass Failure, Mechanics of Material, Finite Element Methods, Correlation Process.

I. INTRODUCTION

Glass failure analysis, particularly integrates glass fractography and microscopy, is a vital tool for diagnosing and identifying the underlying reasons for a breaking or product failure. Analyses must be offered for goods from all industries, including those in the food and beverage packaging, furniture, residential glass, research glassware, and pharmaceutical packaging categories. When utilized properly, glass objects are highly sturdy, yet damage or flaws might result in unexpected failure. Design flaws, poor glass quality, production or processing problems, material interactions, improper handling, or abuse are some of the causes of breakages. It's common for the circumstances around a glass break to be ambiguous. We can identify the true cause of glass failure using the evidence present in the broken sample, which can help solve problems now and, in the future. To

enable a thorough investigation, finite element analysis performed after physical test and additionally, a correlation technique will be used to do the variation investigation [18].

Glass is a stiff, brittle substance that is translucent or clear. It is made by the fusion manufacturing method. Glass is used in design for a multitude of purposes and comes in many different forms [13].

Fig.1 Use of Glass as Building Envelope [13]

The three-point bending flexural test yields figures for the material's flexural stress-strain response as well as the bending modulus of elasticity (Ef), flexural stress (6f), and flexural strain (ef). This test is carried out using a three-point bend fixture or a four-point bend fixture on a universal testing machine (tensile testing machine or tensile tester). The simplicity of the specimen preparation and testing is the principal benefit of a three-point flexural test. The findings of the testing method are susceptible to specimen and loading geometry as well as strain rate, which is a drawback of this method [19].

II. GLASS FAILUER

A. Glass failure analysis under impact loading condition

Zhen Wang, Dayou Ma, Tao Suo, Yulong Li, Andrea Manes in 2021 Three numerical techniques are examined in this study to simulate brittle materials under quasi-static and dynamic stress situations. These methods consist of the elastic bond-based Peri dynamics, the Finite Element Method coupled to Smooth Particle Hydrodynamics, and the Discrete Element Method (DEM) (PD). Numerical models for each technique were produced using LS-DYNA, a commercial piece of software. The parameters pertaining to the mechanical behavior of aluminosilicate glass were calibrated for each numerical model through experimental testing on material coupons. Experimental data from ballistic impact tests and quasi-static three-point bending tests were utilized to evaluate numerical models. The numerical results show the distinct abilities of each strategy to capture the projectile residual velocity and the damage morphology of aluminosilicate glass tiles in ballistic impact scenarios. Under quasi-static flexural stress conditions, all approaches yield results that are equal. But when all loading factors are taken into account, the FEM-SPH method models the mechanical response of aluminosilicate glass the best. [2]

Simulation techniques

The DEM is represented in LS-DYNA by stiff spherical particles. This discontinuous method relies on computing particle motions in accordance with Newton's second rule of motion. Stress and strain fields cannot be directly produced from DEM simulation, unlike other meshfree methods like SPH. Figure 3 displays how the particles adhere to a penalty-based interaction algorithm.

(a). The following is an expression for the interaction distance between two particles:

$$d_{int} = r_1 + r_2 - |\mathbf{x}_1 - \mathbf{x}_2|$$

where r1 and r2 represent the distance between two nearby particles. When dint 0, particles come into mechanical contact with one another, and the standard contact force is specified as.

$$Fn = K_{\mathrm{n}} \mathrm{X}\, d_{\mathrm{int}}$$

$$K_{\mathrm{n}}=((\mathrm{K_1}*\mathrm{r_1}*\mathrm{K_2}*\mathrm{r_2})/(\mathrm{K_1r_1}+\mathrm{K_2r_2}))\ *(\mathrm{NormK})$$

$$Ki = \frac{Ei}{(3) * (1 - 2v)}$$

where the elastic modulus Ei and Possion's ratio I are used to compute the compression modulus of two interacting particles, Ki, and Kn, also known as the normal stiffness coefficient. The penalty function's normal stiffness coefficient is denoted by NormK.

$$Ks = Kn\ X\ ShearK$$

where SheraK is the difference between shear and normal stiffness. All of the DEM simulations in this work used the proposed values of NormK and ShearK, which are 0.01 and 0.286, respectively. This penalty-based particle-particle interaction attribute is defined by the term Control Discrete Element.

The normal coefficient is presented in relation to the tangential constant.

These defined loose particles need to be bonded using the LS-DYNA keyword Define De Bond in order to accurately depict the mechanical behavior of elastic solids. This results in the bonds between all spherical particles being able to transfer tension, shearing, bending, and torsion loads. Microcracks that begin to form in the material might be interpreted as bonds failing at their loading capability.

Consequently, brittle fracture analysis can be performed using this method. The most popular model for simulating brittle fractures is the linear Parallel Bond Model (PBM) in DEM, and it is also the only one included in the most recent release of LS-DYNA (BDFORM=1). The normal force between two bound particles in this paradigm is calculated as

$$\Delta f_n = \frac{PBN}{(r_1 + r_2)} \times A \times \Delta u_n$$

$$A = \pi \times r_{eff}^2$$

$$r_{eff} = \min(r_1, r_2) \times SFA$$

where the effective radius and radius of the two bonded spheres are r1, r2, and reff. The connected spheres' actual contact area is A. The bond radius multiplier, a constant that required to be defined in the keyword, is represented by SFA. The parallel bond normal stiffness is represented by PBN. The relative distance between the two particles in the normal direction is given by the symbol un.

Additionally, you may write down the tangential force between two bound particles as

$$\Delta f_s = PBS \times \frac{PBN}{(r_1 + r_2)} \times A \times \Delta u_s$$

where us is the relative displacement between the two particles in the tangential direction and PBS stands for the parallel bond stiffness ratio (shear stiffness/normal stiffness). Failure parameters must also be established in order to describe the fracture and failure behaviour of brittle materials.

Parallel bond maximum normal stress (PBN S) and parallel bond maximum normal stress (PBS S) are the two failure parameters in PBM [2].

The author tested the impact response of aluminosilicate glass using ballistic penetration. As already seen in Figure 1, a cylindrical projectile with a 10mm diameter and 20mm length was utilized to strike the glass tile (d). During the tests, a plastic sabot covering the bullet was used to optimize the trajectory. As a result, the first surface-to-surface contact between the bullet and glass tile can be ensured. Projectile deflection has a significant impact on both the bullets' residual velocity and the glass tile's behavior during fragmentation. With impact velocities of 84 m/s and 139 m/s, two ballistic experiments were done, yielding projectile residual speeds of 66 m/s and 127 m/s, respectively. The glass tiles were modelled for the subsequent simulation process using various techniques (FEM-SPH, DEM, PD), but the projectile, sabot, and fixture were discretized using finite elements in each case.

T. Pyttel, H. Liebertz, J. Cai in 2010 In case of impact, a laminated glass failure criterion is offered. This criterion's basic tenet is that failure cannot occur unless a critical energy threshold is reached over a finite region. Then, a local Rankine (maximum stress) criterion governs the initiation and propagation of cracks. An explicit finite element solution was used to put the criterion into practice. There is also discussion of several modelling techniques for laminated glass. Numerous experiments with flat and curved laminated glass specimens were conducted to calibrate the criterion and assess its correctness. Finite element simulations were run for each experiment. The criterion's effectiveness is demonstrated by a comparison of measured and simulated results. [3]

There were two sets of tests. Curved and plane safety glass samples were investigated in the first experiment. The experiments with the plane parts were made to reveal details about the main mode of failure and its consequences when impacting laminated glass. Real windshields were used to explore how curvature affected the windshield.

All tests were conducted using a head-impactor from the models in the pedestrian protection family. There is an impactor available.

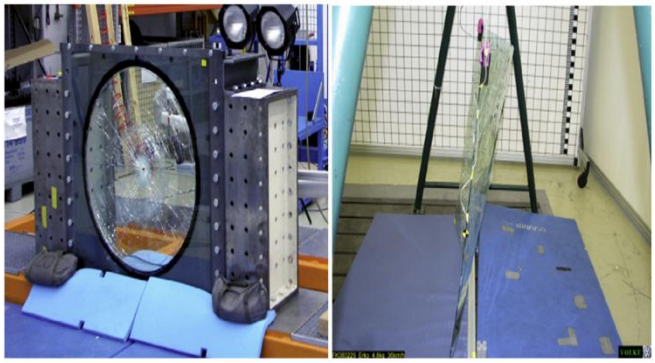

Fig. 2. (Left bounded, right free), Experimental setup for plane parts

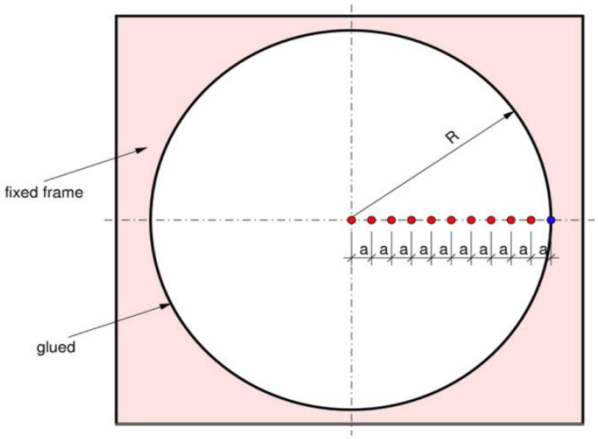

Figure 3 shows the boundary condition and sensor placements for measuring displacement (R: 500 mm, a: 50 mm).

With three various weights (3.5 kg, 4.8 kg and 6.3 kg). Inside the head impactor was a three-axis accelerometer. All of the acceleration measurements for this investigation are conducted using this accelerometer. The experimental setup for plane parts is shown in Fig. 2. A quadratic component is bonded to a circular frame on the left side. As much stiffness as possible was built into the frame. Measurements were made of the glass's deformation and the impactor's internal acceleration. Ten laser extensometers, as indicated in Fig. 3, were employed for this purpose.

The aircraft section was suspended from two cables at the time of the test depicted on the right side of Fig. 2. The stress-free border condition is a benefit of this arrangement. In each of these situations, the part's centre served as the collision point. An overview of the tests conducted using aircraft parts is provided in Table 1. First impactor speed, second impactor weight, and third information regarding boundary conditions make up the test number. For instance, 05 3 b stands for 5.0 m/s, 3.5 kg, and bound.

Automobile manufacturers routinely test their windshields against actual ones to ensure that they will protect passengers or pedestrians in the event of an accident. A safety glass failure model must be able to explain the various phenomena under various loads. Covering the range of impacts to the windshield from outside, inside, and in various locations presents a problem.

Xihong Zhang, Hong Hao, Guowei Ma in 2014 Glass is a material that is always present and is frequently utilized in building façades. People nearby face serious risks from broken glass windows and the glass pieces that result from blast loads and impacts. Understanding glass material properties and simulating glass window reactions to blast and impact loads have received a lot of attention. Therefore, an accurate dynamic constitutive model of annealed float glass, which is frequently used for glass windows, is required for trustworthy predictions of glass structure performances under dynamic loadings. The Johnson Holmquist Ceramic (JH2) model is currently most frequently used to simulate the responses of glass plates to impact and blast loads. This study looks closely at the JH2 model's accuracy in simulating annealed float glass material, particularly under conditions of high strain rate. On soda-lime glass specimens sampled from commonly available annealed float glass panes, static compressive tests and dynamic compressive testing employing Split Hopkinson Pressure Bar (SHPB) are conducted. The model is tested in three different scenarios: a field blasting test on a laminated glass window with dimensions of 1.5 m by 1.2 m; a full-scale laboratory windborne debris impact test on a laminated glass window; and a SHPB compressive test on a glass specimen with dimensions of 15 mm by 15 mm (diameter by length). The simulation results show that the JH2 model with the revised annealed glass material constants makes accurate predictions about how glass and glass windows will react to impact and blast loads. [4]

B. Under Three Point Bending Load

Mingze Ma, Weixing Yao, Wen Jiang, Wei Jin, Yan Chen, Piao Li 2020 In this study, the S-N curves at various stress ratios are produced after the bending fatigue tests of honeycomb sandwich panels are performed utilizing an improved three-point bending test fixture. The honeycomb sandwich panels' failure mode and the source of fatigue damage are identified through the experiment's records of fatigue damage. The causes of the different failure morphologies of the sandwich panels in the L-direction and W-direction are also explained by calculating the shear stress distribution on the honeycomb wall. Additionally, a method for life prediction is suggested, and it has been demonstrated to be useful in foretelling the fatigue life of sandwich panels. [5]

Appendix calculation of stress distribution in sandwich panels.

Consider a sandwich panel that is bending in three directions, as in Fig. 4. Based on beam theory and under the following two presumptions: (1) The shear force and the direction of the shear stress on the cross section are parallel. (2) The shear stress is distributed evenly across the breadth of the section. The analytical aim is chosen to be the section that is L distances from the support end, as shown in Fig 5. The moments on either side of the section are M and M + dM, respectively, within the length dx. M = QL/2. The sandwich panel's neutral layer's curvature is

$$\frac{1}{\rho} = \frac{M}{E_{\mathrm{t}} I_{\mathrm{t}}}$$

where $E_t I_t$ is the equivalent bending stiffness of the sandwich panel, and.

$$E_t I_t = \frac{E_1}{6bt^3} + \frac{E_2}{12bh^3}$$

The normal stresses in the face sheet and the core can be expressed as

$$\sigma_i = \frac{1}{\rho} \cdot yE_i = \frac{ME_i}{E_{\mathrm{t}} I_{\mathrm{t}}} \cdot y, i = 1,2$$

where y is the distance to the neutral layer.The resultant forces on both sides of the section are expressed as

$$F_1 = \sum_{i=1}^{2} \int_{A_i} \sigma_i dA = \int_{A_1} \frac{E_1 M}{E_{\mathrm{t}} I_{\mathrm{t}}} ydA + \int_{A_2} \frac{E_2 M}{E_{\mathrm{t}} I_{\mathrm{t}}} ydA = \frac{M}{E_{\mathrm{t}} I_{\mathrm{t}}} \left(\int_{A_1} E_1 ydA + \int_{A_2} E_2 ydA \right)$$

$$F_2 = \int_{A_1} \frac{E_1 (M + \mathrm{d}M)}{E_t I_{\mathrm{t}}} ydA + \int_{A_2} \frac{E_2 (M + \mathrm{d}M)}{E_{\mathrm{t}} I_{\mathrm{t}}} ydA = \frac{M + \mathrm{d}M}{E_{\mathrm{t}} I_{\mathrm{t}}} \left(\int_{A_1} E_1 ydA + \int_{A_2} E_2 ydA \right)$$

According to the equilibrium equation τ′bdx + F1 = F2 (10) the shear stress can be expressed as

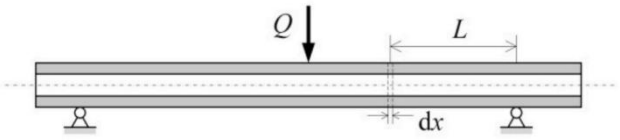

Fig. 4. Sandwich panels under three point bending load.

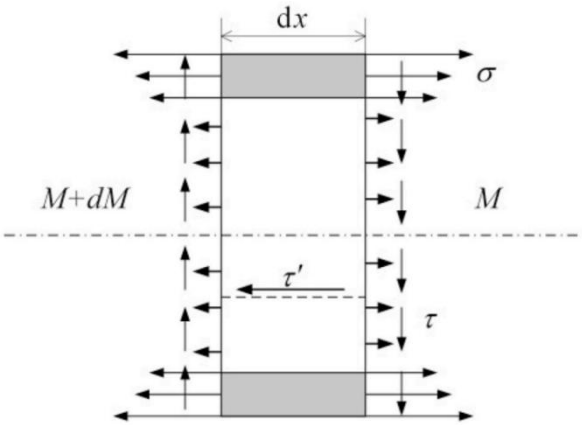

Fig. 5. Stress distribution in face sheet and core

$$\tau' = \frac{\mathrm{d}M}{\mathrm{d}x} \cdot \frac{1}{bE_{\mathrm{t}} I_{\mathrm{t}}} \cdot \left(\int_{A_1} E_1 y \mathrm{d}A + \int_{A_2} E_2 y \mathrm{d}A \right)$$

with

$$\frac{\mathrm{d}M}{\mathrm{d}x} = Q$$

According to the equivalent theorem of shear stress, the shear stress in the face sheet and the core can be obtained as

$$\tau = \begin{cases} \dfrac{E_1(h+t)t}{2E_{\mathrm{t}}I_{\mathrm{t}}} \cdot Q + \dfrac{E_2}{E_{\mathrm{t}}I_{\mathrm{t}}b} \cdot S_z^* Q & \text{in core} \\ \dfrac{E_1}{E_{\mathrm{t}}I_{\mathrm{t}}b} \cdot S_z^* Q & \text{in face} \end{cases}$$

Where S_{z}^* is the static moment of the section, and $S_{\mathrm{z}}^* = \int_{A_i} y \mathrm{d}A, i = 1{,}2$. Since $E_2 \ll E_{\mathrm{t}}I_{\mathrm{t}}$, the normal stress in the core $\sigma_2 = \frac{ME_2}{E_{\mathrm{I_t}}} y \approx 0$. There-

As seen in Fig. 6, select one cell to examine the shear stress on the honeycomb wall. The honeycomb's height is h, its side length is dw, and each cell's wall thickness is w. The L- direction specimen is shown in Fig. 15a. The wall's shear stress is

$$\tau w = \frac{\sqrt{3} * dw * Qc}{2 * b * \delta w * h}$$

The stress distribution on the double-walled honeycomb wall of the W-direction specimen is depicted schematically in Fig. 6c. The double-walled honeycomb wall's actual bearing area is hdw, therefore,

$$\tau_{\mathrm{w}}^{\mathrm{d}} \frac{d_{\mathrm{w}}}{2} h = \tau_{\mathrm{w}}^{\mathrm{s}} \delta_{\mathrm{w}} h$$

then

$$\tau_w^d = \frac{3Q}{bh}$$

$$d_{\mathrm{w}} \gg 2\delta_{\mathrm{w}}, \text{so } \tau_{\mathrm{w}}^{\mathrm{s}} = \frac{3d_{\mathrm{w}}Q}{2b\delta_{\mathrm{w}}h} \gg \tau_{\mathrm{w}}^{\mathrm{d}} = \frac{3Q}{bh}$$

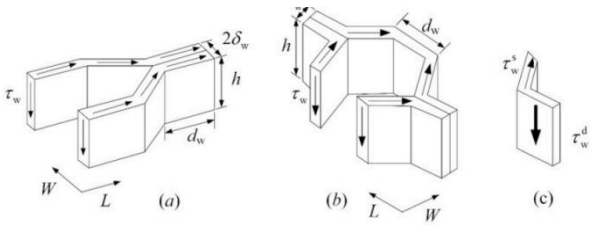

Fig. 6. Stress distribution on the cell wall of honeycomb core.

In this study, the three-point bending fatigue tests of Nomex core honeycomb sandwich panels are performed. The tests and pertinent analysis allow for the following deductions:

- The shear failure of the core is the primary mode of failure of the honeycomb sandwich panel under three-point bending fatigue strain. Failure of the core results in subsequent face sheet fracture and face sheet/core delamination, and the fatigue life of the honeycomb sandwich panels is influenced by the life of the core.

- The morphology of the fatigue failure is substantially influenced by the core orientation. 45 through-thickness cracks typically show up in the L-direction core has smaller crack angles and less continuous cracks than the W-direction core.
- The honeycomb wall's microcracks reveal the fatigue damage in the core, and these microcracks steadily spread throughout the full fatigue life.
- The honeycomb sandwich panel's fatigue life curve can be accurately described by the two-parameter Weibull model over the course of its full lifespan. The core shear stress can be utilized to forecast the fatigue life of the sandwich panel when the core is to blame for the failure of the sandwich panel.
- The stress in the core can be used to estimate the life of sandwich panels, which can make the process of predicting the life of sandwich panels much simpler.

C. Blast loading

Xihong Zhang and Hong Hao in 2016, One of the main reasons for the high number of victims in terrorist bombing attacks and unintentional explosion occurrences has been attributed to the failure of glass windows. To better understand how glass windows react to blast loads and how vulnerable they are, numerous experiments have been conducted. These include the creation of analytical and numerical models to analyze and forecast glass window reactions, as well as laboratory and field studies that have been conducted to experimentally explore glass window performance under explosion scenarios. This article summarizes the research on how glass window systems react to blast loadings. The open literature, which consists of more than 100 papers and materials, is reviewed. Additionally, a brief history and backdrop of relevant studies are provided. We describe our knowledge of the dynamic material properties of glass and the available material models. The accuracy of commonly used analysis techniques and design guidelines for monolithic and laminated glass windows is described. On glass window systems, recent works that include analytical solutions, numerical simulations, and experimental investigations are compiled. A brief discussion of blast-resistant window mitigation strategies is also included. [6]

Xihong Zhang, Hong Hao, Zhongqi Wang in 2014, To lessen the risk from flying glass shards, laminated glass panes are frequently used as blast-resistant glass windows. Either simplified equivalent single degree of freedom (SDOF) analysis or equivalent static analysis are frequently used to forecast how laminated glass windows would react to blast loads. The UFC and ASTM design guides for glass window designs, respectively, similarly use equivalent SDOF and equivalent static analysis. The SDOF study can only forecast the overall responses of glass windows due to inherent issues, and the results are not always accurate. As a result, it is occasionally questioned whether the SDOF analysis is accurate and applicable. For reliable forecasts of laminated glass window responses to blast loads, it is frequently necessary to conduct numerical simulations and/or experimental tests.

To assess the efficacy of available analysis and design methodologies, experimental testing on laminated glass windows subjected to impact and blast loads were conducted in this work. First,

impact tests using a pendulum on laminated panes of various thicknesses were performed. Large-scale field blast tests on laminated glass windows with dimensions of 1.5 m × 1.2 m were conducted. Mechanical linear voltage displacement transducers (LVDT) and high-speed cameras were used to track the deflections of glass panes. In this research, the responses of the examined windows are contrasted with predictions from SDOF models and design guidelines. To assess the correctness of the SDOF and analogous static analyses defined in the design guides, available blast testing data by other researchers are also combined with the current testing data.It is explored if these condensed techniques are adequate for forecasting laminated glass window responses to blast loads. [9]

The central displacement histories of the laminated glass panes were captured by two mechanical LVDT transducers. Transducer probes were affixed to the specimens' centre points made of laminated glass. They tracked the movements of the laminated windows as they redirected into the space and rebounded. Soon after the panes began to rebound, there was debonding between the probes and the broken glass. However, for all of the panes used in the current testing, the greatest centre deflections were noted.

Fig. 7 displays the recorded deflection time histories. High-speed camera images were used to align the time axis so that the deflections only occurred while the blast waves were active. When the probes unbonded from the laminated panes, the deflection histories were condensed. As shown in Fig. 7a, the laminated glass pane gradually distorted under the air blast weaving at first because to the flexural rigidity of the uncracked laminated glass pane. After the glass plies shattered, the laminated pane lost its flexural stiffness, and the deflection quickly increased. For panes 1-1-1 and 1-1-2, the maximum deflections of 275 mm and 280 mm, respectively, were measured at a time of roughly 15 ms, following which the panes started to rebound under the negative pressure. The responses from the other two 7.52 mm laminated panes (2-1-1 and 3-1-1) were comparable to those described previously (Fig. 7b and c). Both of the 7.52 mm laminated panes underwent maximum deflections of 326 mm and 264 mm, respectively, under the blast pressure, before rebounding.

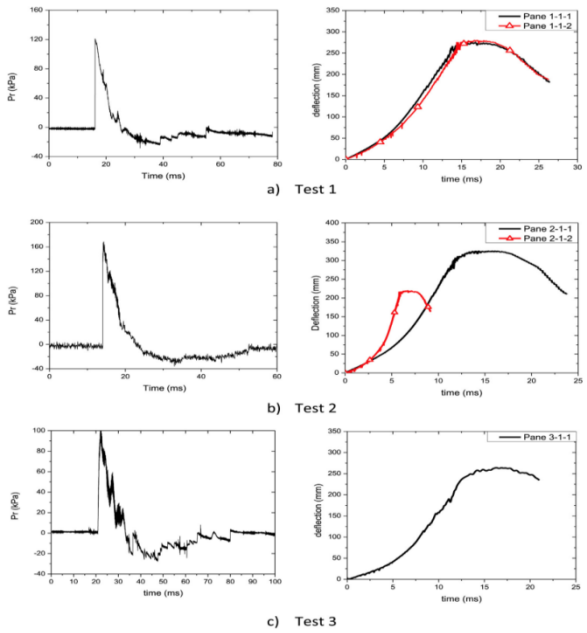

Fig. 7. Recorded reflected pressures and pane deflection histories

The magnitudes of the blast loading were the primary source of the variation in peak deflection. Similar response was also observed in the 13.52 mm laminated pane (2-1-2), but it responded more quickly because of its higher flexural rigidity and smaller maximum central deflection of 220 mm.

Experiments were conducted in this study to examine the responsiveness and blast resistance of laminated glass windows. To assess the window reactions to uniform impact and blast loads, laboratory and field blasting tests were carried out. High-speed cameras were used to track the laminated glass panels' failing process. In the tests, it was possible to quantify the applied impact and blast pressure as well as the dynamic reaction of the window specimens. It was discovered that laminated glass failure happened gradually. The PVB interlayer burst, the exterior glass ply cracked, and the inner glass ply also suffered cracks. Both the PVB interlayer and the inner glass ply cracked. As the glass pane deforms, the cracks on the plies likewise become more numerous. The measured pane central deflection and the pressure histories were utilized to assess the efficacy of the corresponding SDOF analysis and design criteria. It was discovered that the laminated glass answers are underrated by the ASTM standard. When the deflection level is relatively low, the UFC guide and other SDOF-based techniques provide accurate forecasts of the responses of glass windows. The accuracy of the comparable SDOF analysis varies under blast loading with significant panel deflection. The majority of SDOF models undervalue the responses of glass panels, whereas Morison's model with a modified resistance function that takes into account the low resistance and high ductility of PVB material and the deflection dependent load-mass factor produces better predictions but overvalues the responses. The PeI diagrams proposed by others or created based on other methodologies were also compared with the existing and available testing data acquired by other researchers. It was discovered that PeI diagrams created using similar SODF analysis typically underestimate the laminated glass windows' capacity for blast resistance. PeI diagrams can be produced by numerical simulations that are more realistic, but the simulations should take into account how the glass pane will fail when removed from its support.

D. Fracture

Liang Xue, Yuling Niu, Hohyung Lee, Da Yu, Satish Chaparala, Seungbae Park in 2013. Investigation of glass fracture under dynamic impact loading is important because glass must be able to withstand scratches, drops, impacts, and bumps from daily use. Glass has a far higher strength under dynamic fracture conditions than it does under quasi-static force. Numerous theoretical models exist. An accumulated damage model is used in this investigation. Investigation is done into the relationship between stress, loading rate, contact time, and fracture. The dynamic fracture criterion for glass has been shown to be further improved by the effects of impact area, impact energy, and impact momentum on the glass fracture. The first principal strain of the glass during the impact process can be obtained for the experimental research using the Digital Image Correlation (DIC) approach. Additionally, ANSYS/LS-DYNA is used to construct the FEA model. [10]

The effectiveness of the DIC optical technique utilized in the development of glass products is shown. This type of analysis is typically conducted using a strain gauge, but the novel method

would have additional benefits. The fact that the specimen is not in contact, the capability of directly calculating strain values, and the capacity to record the dynamic impact reaction at a very high frequency are some of the benefits. The use of DIC techniques also makes it possible to have excellent resolution across a tiny region.

The deflection and strain experienced by the glass panels during the ball drop impact test are measured using the DIC. The data and projections had excellent agreement when it came to maximum deformation.

Higher drop energies result in a shorter time to failure. With higher drop energies, the loading rate rises. It demonstrates how closely the dynamic fracture and fracture time are related. In order to depict the dynamic fracture, momentum change is suggested as a parameter.

Under dynamic impact loading, the glass will shatter into long strip debris. Because the glass is prevented from shattering at flaws caused by surface defects by the layer with high compressive stress.

The glass exhibits a similar fracture surface to conventional glass, according to the SEM micrographs. In our situation, a second mist zone was created, however this was presumably due to the glass' manufacture procedure.

The larger the steel ball, the greater the shift in momentum it experiences, which accounts for the longer time it takes for the huge steel ball to separate from the glass panel after impact.

To determine how they affect the fracture of the glass, experiments in which projectiles of various shapes and materials impact the glass must be carried out. Another intriguing topic is how the dimension of glass affects the strength of glass.

Luigi Biolzi, Sara Cattaneo, Gianpaolo Rosati, in 2009, The development of transparent load-bearing parts for architectural glazing applications has increased the use of laminated glass. To enhance the glass's post-breakage properties, laminated glass combines two or more layers of glass with thin thermoplastic interlayers. The laminate's residual load-carrying capability after breakage is based on the mechanical characteristics of its component parts. On laminated glass specimens constructed of two equal external panels of tempered glass and an internal panel of float glass, three-point bending tests are shown. Three different combinations of annealed float and fully thermally tempered glass plies were used to distinguish the laminated glass specimens, which had equal cross sections. Additionally, two distinct interlayers with drastically varied mechanical properties were used to build two sets of specimens. The tests were run at room temperature with the flexural load parallel to the laminate plane (in-plane loading). The failure mechanisms discovered as well as the post-failure response are presented and discussed. [11]

The structural performance and failure modes of laminated glass beams under in-plane loads were tested at various ambient temperatures, and the findings and observations from those tests were described in this work. These inferences can be made in light of the research:

In plane loaded, layered beams' flexural response is significantly influenced by the interlayer. In contrast to what has been observed for laminated glass/PVB beams, gradual failure has been

identified for laminated glass/SGP beams. As a result, the interlayer's quality is a factor in the post cracking range. Glass beams also have a high degree of slenderness for lateral torsion buckling. Although initial tests for the laminated glass/SGP beams did not indicate any issues with lateral stability for laminated glass beams/PVB beams, it was essential to prevent instability with X-bracing in this situation. Although in real applications additional components frequently inhibit lateral stability, an SGP interlayer's significantly improved stiffness properties may have a significant impact on buckling stresses. In any case, the characteristics of both the PVB and SGP interlayer exhibit susceptibility to creep under long-term loadings and temperature dependent response, which results in the laminated beams having a time and temperature dependent behavior.

Glass laminated beams exhibit drastically different flexure and fracture behavior from monolithic glass beams and exhibit several structural conditions:

- The annealed float glass ply was the first to break;
- the response was essentially linear with potential follow-up localized cracks (with SGP interlayer) before an abrupt fragmentation of both exterior glass plies.
- Large deformations and shattering of the polymer interlayer, with total loss of the laminated beam's load-bearing capability

The results of the numerical analyses and the experiments demonstrated that even when a laminated glass beam is loaded perpendicular to the lamination plane (in-plane loading), an interlayer with increased stiffness activates the presence of an annealed float glass phase even in a cracked stage, stiffening the structural system, raising the collapse load, and providing a higher residual strength by adding beneficial effects to improving the flexural-torsional stability.

III. ILLUSTRATION TO THREE POINT LOADIND CONDITION

Three Point Bend Test

The three-point bending flexural test yields figures for the material's flexural stress-strain response as well as the bending modulus of elasticity (Ef), flexural stress (6f), and flexural strain (ef). This test is carried out using a three-point bend fixture or a four-point bend fixture on a universal testing machine (tensile testing machine or tensile tester). The simplicity of the specimen preparation and testing is the principal benefit of a three-point flexural test. The findings of the testing method are susceptible to specimen and loading geometry as well as strain rate, which is a drawback of this method.

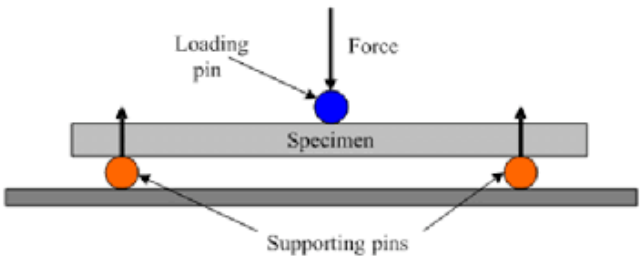

Fig.8 Three Point Bend Test [15]

The test is typically performed using a designated test fixture on a universal testing equipment. The preparation, conditioning, and conduct of the test have an impact on the test results. The sample is positioned between two pins that are used as supports[19].

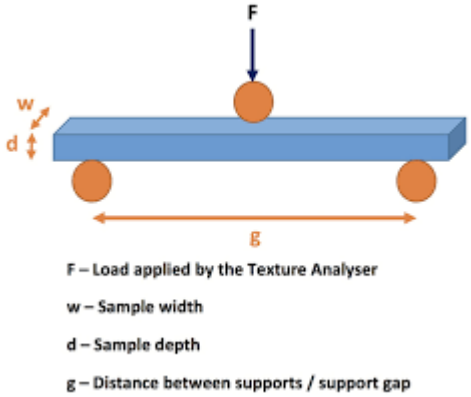

Fig.9 Illustration of Three Point Bend Test [16]

IV. Conclusion

Most of the journal were reviewed and different test on glass were illustrated on Impact, under three Point Loading, Blasting & fracture on the glass, each of the results shows different criteria of failing with its loading condition FEA software's and other CEA software helps in testing the failure criteria with minimum cost on testing. Hence the paper reviewed are sorted with results.

This review article helps in determining the various types of failure of glass under different loading condition, to know the fracture ratio of different glass material with its boundary's one can research most unique way to strengthen the glass with this application to its failure with this article.

References

[1] Xihong Zhang, Hong Hao, Guowei Ma. Parametric study of laminated glass window response to blast loads. Engineering Structures, 2013. doi.org/10.1016/j.engstruct.2013.08.007.

[2] Zhen Wang, Dayou Ma, Tao Suo, Yulong Li, Andrea Manes. Investigation into different numerical methods in predicting the response of aluminosilicate glass under quasi-static and impact loading conditions. International Journal of Mechanical Sciences, 2021. doi.org/10.1016/j.ijmecsci.2021.106286.

[3] T. Pyttel, H. Liebertz, J. Cai. Failure criterion for laminated glass under impact loading and its application in finite element simulation. International Journal of Impact Engineering, 2010. doi.org/10.1016/j.ijimpeng.2010.10.035.

[4] Xihong Zhang, Hong Hao, Guowei Ma. Dynamic material model of annealed soda-lime glass, International Journal of Impact Engineering, 2014. doi.org/10.1016/j.ijimpeng.2014.11.016.

[5] Mingze Ma, Weixing Yao, Wen Jiang, Wei Jin, Yan Chen, Piao Li. Fatigue Behavior of Composite Sandwich Panels Under Three Point Bending Load. Polymer Testing, 2020. doi.org/10.1016/j.polymertesting.2020.106795.

[6] Xihong Zhang and Hong Hao. The response of glass window systems to blast loadings: An overview. International Journal of Protective Structures, 2016. DOI: 10.1177/2041419615626061.

[7] Xing-er Wang, Jian Yang, Feiliang Wang, Qingfeng Liu, Han Xu. Simulating the impact damage of laminated glass considering mixed mode de-lamination using FEM/DEM. Composite Structures, 2018. doi.org/10.1016/j.compstruct.2018.05.127.

[8] Hong-Seok Kim, Byung-Kuk Ha, Bum-yul Yoo, Ho-Seung Jeong, Sang-Hu Park. Numerical prediction of dynamic fracture strength of edge-mounted non-symmetric tempered glass panels under steel ball drop impact. Journal of Materials Research & Technology, 2022. doi.org/10.1016/j.jmrt.2021.12.134.

[9] Sai Pandraju, T. K., Samal, S., Saravanakumar, R., Yaseen, S. M., Nandal, R., & Dhabliya, D. (2022). Advanced metering infrastructure for low voltage distribution system in smart grid based monitoring applications. Sustainable Computing: Informatics and Systems, 35 doi:10.1016/j.suscom.2022.100691

[10] Sharma, R., & Dhabliya, D. (2019). A review of automatic irrigation system through IoT. International Journal of Control and Automation, 12(6 Special Issue), 24-29. Retrieved from www.scopus.com

[11] Xihong Zhang, Hong Hao, Zhongqi Wang. Experimental study of laminated glass window responses under impulsive and blast loading. International Journal of Impact Engineering, 2014. doi.org/10.1016/j.ijimpeng.2014.11.020.

[12] Liang Xue, Yuling Niu, Hohyung Lee, Da Yu, Satish Chaparala, Seungbae Park. An experimental and numerical study of the dynamic fracture of glass. International Technical Conference and Exhibition on Packaging and Integration of Electronic and Photonic Microsystems, 2013. IPACK2013-73292.

[13] Luigi Biolzi, Sara Cattaneo, Gianpaolo Rosati. Progressive damage and fracture of laminated glass beams. Construction and Building Materials, 2009. doi:10.1016/j.conbuildmat.2009.09.007.

[14]]https://www.which.co.uk/news/article/exploding-ovens-why-glass-doors-shatter-andwhat-to-do-it-if-happens-to-you-a7Hyv3G8IxcT

[15] https://theconstructor.org/building/types-glass-properties-applications-construction/14755/#Engineering_Properties_of_Glass

[16] https://thedesignbridge.in/blog/glass-properties-types-material-performances-and-uses-in-construction/

[17] https://www.researchgate.net/publication/264713313/figure/fig1/AS:295937667813388@1447568446962/Three-point-bending-test-8.png

[18] https://3.bp.blogspot.com/ XzdizWYCSkY/W46owsCbCzI/AAAAAAAAGXg/ZZ4Aq-pXNWA5Aj79uHakg1b-q1uZ8DxfwCLcBGAs/s1600/graph15.jpg

[19] https://www.researchgate.net/profile/Franz Poelzl/publication/313662114/figure/fig50/AS:668718371700761@1536446292974/Stress-strain-curves-of-steel-and-glass-for-an-uniaxial-tensile-loading-scenario-redrawn.png

[20] https://www.glass-ts.com/services/glass-failure-analysis/

[21] https://en.wikipedia.org/wiki/Three-point_flexural_test

[22] https://www.vitroglazings.com/media/d4wbnqbh/vitro-td-110.pdf

[23] Veer F, Zuidema J, Bos FP. The strength and failure of glass in bending. Glass processing days; 2005. p. 1–3.

[24] Girija Vallabhan CV, Das YC, Ramasamudra M. Properties of PVB interlayer used in laminated glass. J Mater Civil Eng, ASCE 1992;4(1):71–7.

[25] Minor JE, Reznik PL. Failure strengths of laminated glass. J Struct Eng, ASCE 1990;116(4):1030–9.